KAULA, W.M.
Department of Planetary & Space Science
University of California
Los Angeles, California 90024
United States of America

Proc.Symposium on Earth's Gravitational Field & Secular Variations in Position (1973),410-412.

GEOPHYSICAL IMPLICATIONS OF LUNAR LASER RANGING

ABSTRACT

Laser distance measurements to the Apollo retroreflector packages are currently being made regularly by the McDonald Observatory with an accuracy of 15 cm. A new station being constructed on Maui has an accuracy goal of 2 or 3 cm. The results over two and a half years have been fit with an accuracy of 3 m. Improvements in the theory of the moon's angular motion about its centre of mass and in lunar orbit calculations are expected to give better agreement between theory and experiment soon. Future results are expected to include measurement of polar motion to a few cm, UT-1 to 100 microsec, and crustal movement to a few cm. Repeated station location measurements with a mobile station at a network of fundamental sites spaced perhaps 1000 km apart, when supplemented by accurate absolute gravity measurements, seem capable of providing a reliable reference framework for the measurement of the dynamics of the Earth's crust and upper mantle.

1. Text

This paper is a team report. The report by BENDER ET AL (1973)* covers developments till early 1973. This paper brings that report up-to-date and discusses some of the predicted applications for geophysical uses.

The instrumental jitter is ±2½ nsec or ±50 cm in range. A normal point obtained from a 15 min. span has an uncertainty of ±15 cm in range from the telescope to the retro-reflector on the moon. A three parameter (the position of the moon with respect to the telescope) fit of 5 or 6 hours of data has an rms residual of ±11 cm. So it would appear that the data itself has an accuracy of ±15 cm.

From the point of view of the data analyst, the main objection is that the data are not a completely continuous record. In a typical month, there are data for only 14 days. The gaps in the data are 9 days (around new moon), 2 days, and two of 1 day each. As with artificial satellite tracking, these gaps in the data contribute much more to uncertainty in the results than the instrumental inaccuracy.

As discussed by BENDER ET AL (1973), considerable progress has been made. The best information available in 1969 leads to residuals of several hundred metres. A solution for a reasonable number of parameters (21) enables the residuals to be brought down below ±3 m for a three year long data record. Since BENDER ET AL (1973), when it was felt that the main reason for the ±3 m were the physical librations, a new model for the physical librations has been generated by Eckhardt considering the third degree harmonic terms and the non-linear iteration terms. The present situation

* copies distributed to symposium participants

for a long data span is about ±0.5 m for the relative position of the retro-reflectors and ±1 m for the orbital error.

The ±1 m residual also depends on a tidal acceleration of 38 sec per century^2, confirming the values found by other techniques in recent years.

The current modeling work, mainly by J.G. Williams, is trying to work out some discrepancies between numerical integration and iteration theories in the physical librations. The ±1 m error does not prevent much smaller geophysical effects from showing up. Discrepancies between two points on the same day, e.g., errors in UT1 and in the polar wobble, are caused by differences in range at different times of day for the same station. These effects are at the 0.2 m level, smaller than the estimate of the accuracy of the BIH pole position (0.4 m).

Error analyses (KAULA 1973) confirm that the spectral separation by the Earth's rotation enables determination of geophysical and geodetic parameters to much smaller uncertainties than the total uncertainty of the system. The following are some results from error analyses of hypothetical spans for 440 days of data. ±15 cm instrumental uncertainty was assumed, and 97 parameters were solved for.

Stations in Texas & Hawaii, plus: -				Australia	Crimea	Azores
Station Drift	E-W cm/yr /yr	-	4.5	4.1	4.4	4.4
	N-S cm/yr	-	25	18	19	20
Wobble	13.25d cm	-	2.6	1.5	1.5	1.6
	13.66 cm	-	3.8	1.8	1.9	2.1
	14.11 cm	-	3.0	1.7	1.6	1.9
	27.33d cm	-	5.6	2.8	3.7	3.1
Rotation	13.25d 10^{-6}s	-	18	10	9	11
	13.66 10^{-6}s	-	34	20	22	24
	14.11 10^{-6}s	-	21	13	12	14
	27.33d 10^{-6}s	-	211	80	128	159
Tidal Love No.	h	-	-	0.60	0.29	0.49	0.44

The reason why east-west drift is so much better determined than north-south drift is that the effect of station drift on the signal will be sinusoidal with a period of 24 hours; the phase depends on longitude and the amplitude depends on the distance from the rotation axis. The error ellipsoid for position determination from laser ranging has its longest axis parallel to the rotation axis and its shortest in the longitude direction.

The main weaknesses in the error analysis are the truncated rotation and wobble spectra and the assumption of day-to-day randomness of gaps in the data. However, it is evident that the main need is a southern hemisphere station to get better coverage of the orbit, as well as more sensitivity to polar wobble.

2. References

BENDER, P.L., CURRIE, D.G., DICKE, R.H., ECKHARDT, D.H., FALLER, J.E., KAULA, W.M., MULHOLLAND, J.D., PLOTKIN, H.H., POULTNEY, S.K., SILVERBERG, E.C., WILKINSON, D.T., WILLIAMS, J.G. & ALLEY, C.O. 1973. The Lunar Laser Ranging Experiment. *Science* 182,229-238.

KAULA, W.M. 1973. Potentialities of Lunar Laser Ranging for Measuring Tectonic Motions. *Phil.Trans.R.Soc.Lond.A* 274,185-193.

3. Discussion

HOLDAHL: You mentioned a 1000 km spacing for observing stations. Do you think a spacing of VLBI or Lunar Laser Ranging stations of less than 1000 km would produce greater advantages than have already been obtained by use of current terrestrial methods?

KAULA: I referred to one of laser ranging to satellites and the moon or VLBI. All three might have a certain role, but the global role of lunar ranging or VLBI or the regional role of satellites involve many obstacles that have to be dealt with. From the point of view of geophysics and the determination of secular motion, regional determinations are more important than long wave determinations of secular motion.

MUELLER: On the last slide that you showed were there three stations observing four reflectors?

KAULA: Two reflectors. There were two and the three stations adding on to the Hawaii station, the third station. The table was published in (KAULA 1973). A similar analysis has also been made by Counselman. Bender has also made an analysis, which was not a conventional error analysis but defines systematic error contributions.

Proc. Symposium on Earth's Gravitational Field & Secular Variations in Position (1973), 413-432.

LUCK, J. McK.
MILLER, M.J.
MORGAN, P.J.
Division of National Mapping
Department of Minerals & Energy
Canberra ACT
A U S T R A L I A

THE NATIONAL MAPPING LUNAR LASER PROGRAM

ABSTRACT

National Mapping is reassembling the AFCRL Laser Ranger at Orroral in the ACT for the purpose of Laser Ranging. The site was chosen after a careful examination of many factors including number of clear/usable nights, 50%; level of precipitable water vapour, less than 10 mms; level of logistical support available, high; night sky contamination assessed as zero and average atmospheric seeing quality, normally less than 2 arc seconds. The determination of the site and the granting of the necessary approvals is now complete after almost nine months of continuous activity.

The proposed configuration of the hardware is to use a modified cassegrain (Nasmyth) focus position of a 1.5 metre astronomical telescope to transmit and receive photons generated by a 4 stage ruby laser operating initially with a power of 3 Joules, once every five seconds with a 10 nanosecond pulse width. Plans are in hand to reduce the pulse width as expertise becomes available. Timing will be at the one nanosecond level, consequently the initial limitation will be due to pulse length.

Tracking will be accomplished by a servo-loop working from the main field optics and an image dissecting tube with a digital step size of 0.6 arc seconds to both the equatorial and declination axis. A feature of the system is the ability to track on a lunar object, usually a region of high contrast, and then to offset from a known lunar point to the retroreflecter which corresponds to the optical axis of the system.

The object of this program is to monitor the secular changes in position that occur as a direct result of: variations in the rotational speed of the earth and its inclination, commonly referred to as polar motion; crustal motion, commonly referred to as continental drift, and hopefully, long term changes in gravitation, tidal coupling and the variation of astronomical constants.

1. Introduction

To augment its programs of studying secular geodetic changes and monitoring polar motion, the Division of National Mapping is installing a Lunar Laser Ranger (LLR) at Orroral Valley in the Australian Capital Territory. It consists of a 150 cm Ritchey-Chretien telescope used in the modified Cassegrain (Nasmyth) configuration, a one gigawatt pulsed ruby laser, a minicomputer for telescope and laser control and data acquisition, and associated control electronics.

The equipment was made available to the Division as a long term loan from NASA in cooperation with the Smithsonian Astrophysical Observatory. It was formerly operated by the US Air Force Cambridge Research Laboratories at Mount Lemmon in Arizona.

Briefly, its principle of operation is to fire a laser pulse three nanoseconds long through the telescope which collimates the pulse to 2 arc seconds of beam divergence. The pulse impinges on one of the retroreflectors placed on the Moon's surface by Apollo astronauts and returns through the telescope

to a pulse detector which stops a nanosecond counter started by the outgoing pulse. Twice the telescope-retroreflector distance is therefore measured in terms of the velocity of light.

A minimum set of three observatories well separated in latitude and longitude, and three lunar retroreflectors well separated in selenocentric latitude and longitude will, if operated simultaneously or in cooperation over an extended time period, permit the determination of the vectors GT, GM, MR, (figure 1) relative to an inertial reference frame for each of the stations and each of the retroreflectors.

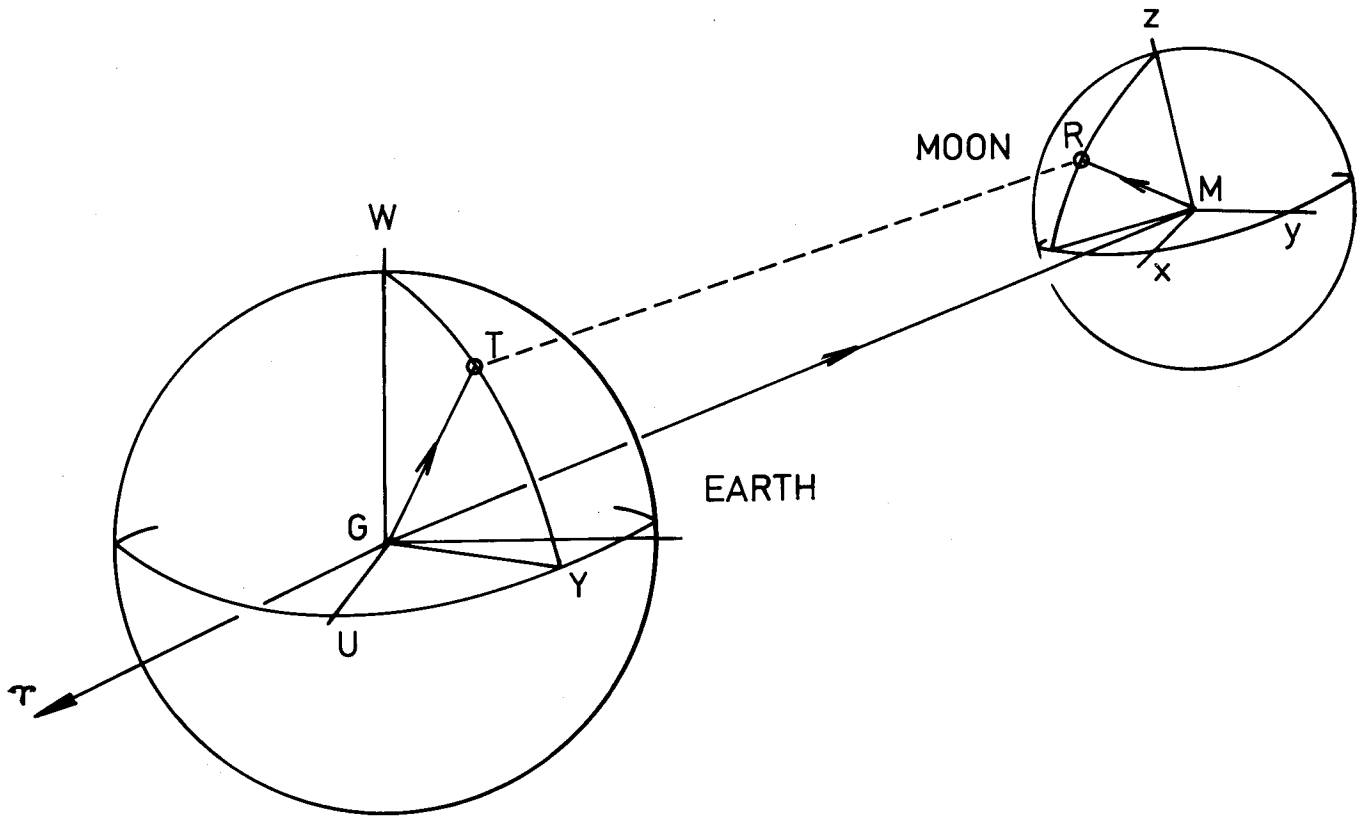

Figure 1.
Earth-Moon System

2. Site Selection and Preparation

Prime site requirements are geologically stable bedrock foundations, clear sky and good seeing, and low precipitable water vapour. Logistics is an important consideration in view of the limited budget available.

2.1 Region

The US agencies concerned require that the LLR be located in Australia for Geodetic reasons. A study of the geology of Australia showed that the ACT was a suitable location. It was early recognised that placing the LLR in reasonable proximity to the Mount Stromlo Photographic Zenith Tube (PZT) would provide a unique opportunity for comparing two entirely different techniques in measuring the polar motion and, indeed, continental drift, while similar comparisons against Very Long Baseline Interferometry would be feasible if the LLR were close to radio telescopes which exist at tracking stations in the ACT. The Division's general interest in earth satellite tracking by Doppler methods and foreseeably by laser satellite tracking reinforced the desirability of the ACT as a site. Finally, the convenience of proximity to Head Office was not ignored.

A possible site at Siding Spring in northern NSW, adjacent to the Anglo Australian 150 inch telescope was considered. While the percentage of clear nights per year there is undoubtedly greater than in the ACT, it lacks geodetic and positional astronomy facilities, is remote, and is inferior to the ACT in freedom from precipitable water vapour.

2.2 Precipitable Water Vapour

Since the wavelength, $6943A^{o}$, of the emitted ruby laser pulse is close to an atmospheric water vapour absorption band, it is an operational requirement that the level of precipitable water vapour in the atmosphere be minimum, less than 10mm for optimum performance.

Firstly, a comparative study was made of the monthly mean values of water vapour in the Coonabarabran (Siding Spring) and Canberra regions using relative humidity data supplied by the Canberra Bureau of Meteorology, and a formula (REITAN 1963) for converting monthly mean dewpoints $D^{o}F$ to total precipitable water vapour at sea level, u:

$$\ln u = -0.981 + 0.0341\ D$$

Table 1 shows that the Canberra region is superior in this respect, even more so considering the fact that Canberra has considerably more rainy days than Coonabarabran. Studies at Mount Stromlo Observatory by HYLAND (1973) indicate that on clear nights there the frequency distribution of precipitable water vapour ranges from 4 to 18 mm and peaks at 6 to 8 mm.

Secondly, daily radiosonde data acquired in 1971-2 by the Bureau of Meteorology at its Wagga, NSW, station were analysed to give the total precipitable water vapour profile against pressure (altitude). The other nearest station is at Nowra, NSW, but as it is a coastal station it was considered unsuitable for either comparison or averaging; the Bureau considered that the Wagga data was suitable for our purposes, especially as the mean motion of the sonde is towards Canberra.

From the wet and dry bulb temperatures and pressure profiles obtained from the radiosondes, the mixing ratios m(z), defined as the ratios of the mass of water vapour to the mass of dry air at altitude z, were read from aerological diagrams at various pressures. Now the pressure p(z) at altitude z is given by

$$p(z) = -\int_z^\infty g\rho(x)dx$$

where $\rho(x)$ is the density at height x. Also, the amount of water vapour in a volume element $A\delta z$ at height z is

$$\delta w(z) = m(z)\rho(z)A\delta z$$

whence

$$W(\infty) - w(h) = \frac{A}{g}\int_{p(h)}^{\infty} m(z)dp(z)$$

Since $W(\infty) = 0$, the total precipitable water vapour above unit surface at height h, i.e. $w(h)/A$, was obtained by simple numerical integration. Typically, after converting to pressure, w(950 mbar) - w(850 mbar) = 5mm. The altitude of the collimation tower site at Orroral Valley tracking station, 1400 metres, corresponds approximately to a pressure of 850 mbar; the mean monthly results subdivided by class of cloud cover are given in table II.

TABLE I

Comparison of Precipitable Water Vapour

Canberra and Coonabarabran

Monthly Mean Precipitable Water Vapour at Sea Level (u mm), by Formula (REITAN 19)					
Month	Canberra	C'bran	Month	Canberra	C'bran
Jan	21.4	25.3	Jul	14.6	16.3
Feb	23.6	26.1	Aug	14.6	15.7
Mar	20.5	24.6	Sep	16.3	16.3
Apr	19.3	22.0	Oct	16.8	18.0
May	16.8	18.6	Nov	19.9	21.4
Jun	15.2	16.8	Dec	20.5	23.6

TABLE II

Precipitable Water Vapour - Canberra

Precipitable water vapour (mm) Canberra region, 1972, altitude 1400 metres							
Month	Cloud Cover 0/8-2/8	3/8-5/8	6/8-8/8	Month	Cloud Cover 0/8-2/8	3/8-5/8	6/8-8/8
Jan	9.7	10.5	13.5	Jul	4.5	7.4	6.0
Feb	14.9	12.4	15.1	Aug	5.2	4.5	5.6
Mar	14.0	14.5	13.3	Sep	5.5	4.9	6.9
Apr	8.8	7.4	8.4	Oct	6.0	7.5	4.8
May	7.4	8.4	7.3	Nov	9.0	7.5	10.0
Jun	5.1	3.3	5.6	Dec	6.4	5.7	8.6

2.3 Cloud Cover

The Bureau of Meteorology and Mount Stromlo Observatory made available their observations of cloud cover at various times of every day in the period June 1970 to December 197 2. The observations at Fairbairn Airport, Canberra, were made professionally every three hours; at Mount Stromlo Observatory by the regular night assistants at 9 pm, midnight and 3 am; and at other stations, at 9 am and 3 pm. The comparison between Mount Stromlo and Orroral Valley uses the Fairbairn data set as an interpolator. Table III shows the percentage of days in the period having each of three classes of cloud cover at each station. Note that Yarralumla is very close to Mount Stromlo. Table IV gives the monthly values for Orroral Valley at 9 am and 3 pm. The Division's own informal observations suggest that, at night, the incidence of cloud cover may be even less than the tables indicate.

TABLE III

Cloud Cover - Comparison

Percentage of days with given cloud cover, 1970-2

Time	Station	0/8-2/8	3/8-5/8	6/8-8/8
9 am	Orroral Valley	42	17	41
	Fairbairn	35	18	47
	Yarralumla	35	15	50
3 pm	Orroral Valley	33	22	45
	Fairbairn	30	26	44
	Yarralumla	31	23	46
9 pm	Fairbairn	47	20	33
	Mt Stromlo	40	13	47
Midnight	Fairbairn	47	15	38
	Mt Stromlo	38	11	51

TABLE IV

Cloud Cover - Orroral Valley

Percentage of Days with Given Cloud Cover, Orroral Valley, ACT

Month	Period Averaged	9am			3pm		
		0/8-2/8	3/8-5/8	6/8-8/8	0/8-2/8	3/8-5/8	6/8-8/8
Jan	1971-2	28	13	59	16	27	57
Feb	1971-2	28	16	56	18	24	58
Mar	1971-2	29	16	55	31	25	44
Apr	1971-2	47	15	38	47	18	35
May	1971-2	42	18	40	36	20	44
Jun	1972	64	7	29	53	14	33
Jul	1970-2	53	11	36	46	24	30
Aug	1970-2	32	25	43	25	25	50
Sep	1970-2	47	18	35	40	21	39
Oct	1970-2	50	20	30	34	26	40
Nov	1970-2	40	20	40	27	22	51
Dec	1970-1	47	19	34	38	25	37

In summary, the Orroral site is superior to a Mount Stromlo site in both cloud cover and precipitable water vapour aspects.

2.4 Seeing and Fog

An 8 inch reflecting telescope was tested against the Oddie telescope at Mount Stromlo and taken to Orroral where, on several nights, double stars of close separation were observed to assess the seeing. The operational requirement of the LLR is that, to achieve the desired pointing accuracy and signal-to-noise ratio, the beam direction and beam divergence should be stable to better than two arcseconds. On each occasion double stars of separation less than 1".5 were readily resolved. MEINEL (1963) indicates that, in testing for a medium large telescope, a test aperture of at least 10 cm is required so that the large scale blurring effect characteristic of seeing disturbances in large telescopes is observed rather than mere image motion observed by small telescopes.

An interesting point is that, in general, the seeing at the collimation tower was much superior to the seeing on the valley floor 400 metres below.

The site is situated on a level part of the slope of Mount Orroral, as in figure 2. It is expected that deterioration of the seeing as the air flow encounters a knoll (KIEPENHEUER 1962) will not be serious as the knolling is small and the telescope will be 28 feet above ground level.

Advantage was taken of the valley profile (figure 2) to determine the height of the inversion layer above the valley floor. On two nights, one clear and the other with fog in the valley, observations of wet and dry bulb temperatures and barometric pressure were taken at regular intervals both across the valley and along it. The graphs of dry temperature against scale height, shown normalised in figures 3 and 4, clearly indicate that the normal inversion layer lies well below the collimation tower. This is confirmed by the fact that not once during 1973 was there fog at that site.

2.5 Geological Surveys

An extensive series of seismic and resistivity tests of both valley and collimation tower sites was conducted by the Bureau of Mineral Resources to verify the geodetic stability of the sites. (The valley floor was included as it was a logistically desirable site). Figure 5 is a plan of the geophone arrays used in the seismic survey at the tower site, and figure 6 shows the bedrock profiles relative to the surface. A massive bedrock outcrop with a 30 foot diameter flat top was chosen as the prime area of interest; the tests established that, within interpretable limits, the outcrop was at the very worst, a large tor sitting solidly on bedrock and surrounded by highly weathered granitic material. Electrical resistivity tests confirmed this finding. The valley floor site was not so suitable, bedrock there being some 10 metres from the surface in all cases.

2.6 Logistics

Within the ACT, Mount Stromlo is undoubtedly the best site from the point of view of access, proximity to Head Office, and building and technical services, water, power and communications facilities.

Access to the Orroral collimation tower site is possible through a locked gate under most weather conditions in four-wheel drive vehicles; it has standard US configured power and telephone readily available, but no water. It is within reasonable daily travelling distance from Canberra, and is collocated with a major technical facility, the Orroral Valley STDN Tracking Station.

For the preceding reasons, the tower site has been chosen for erection of the LLR.

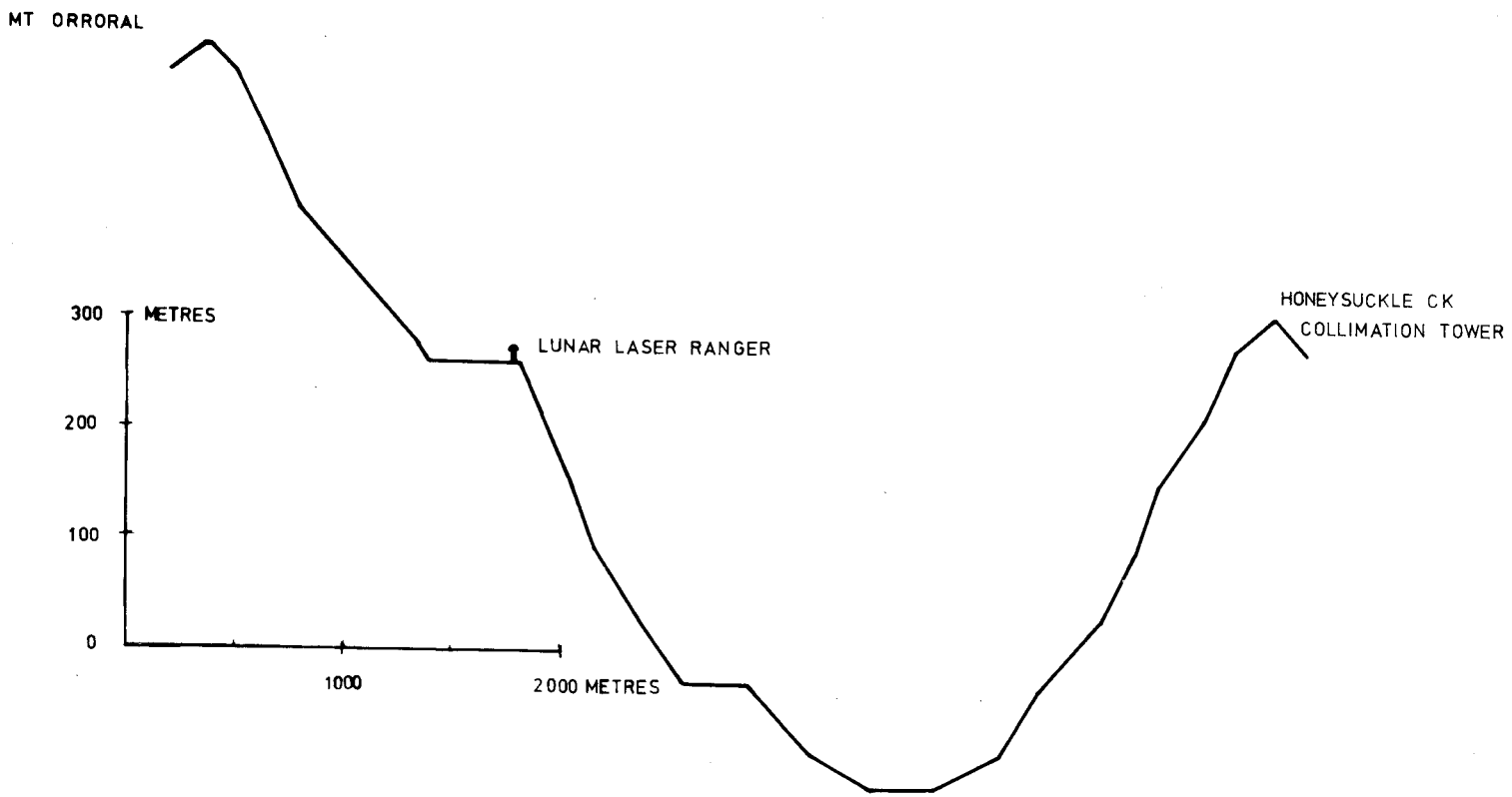

Figure 2. Longitudinal Section Across Orroral Valley

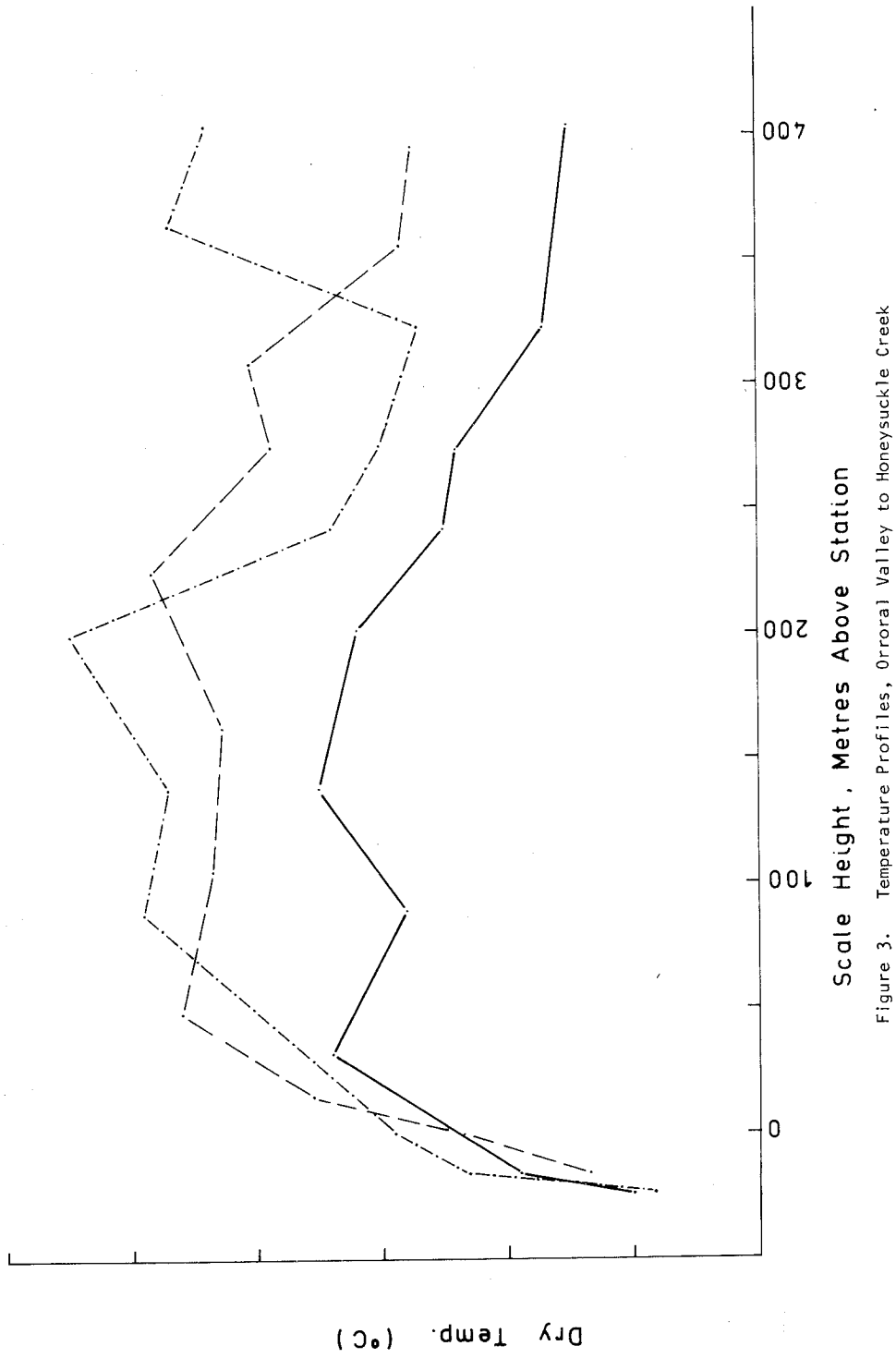

Figure 3. Temperature Profiles, Orroral Valley to Honeysuckle Creek

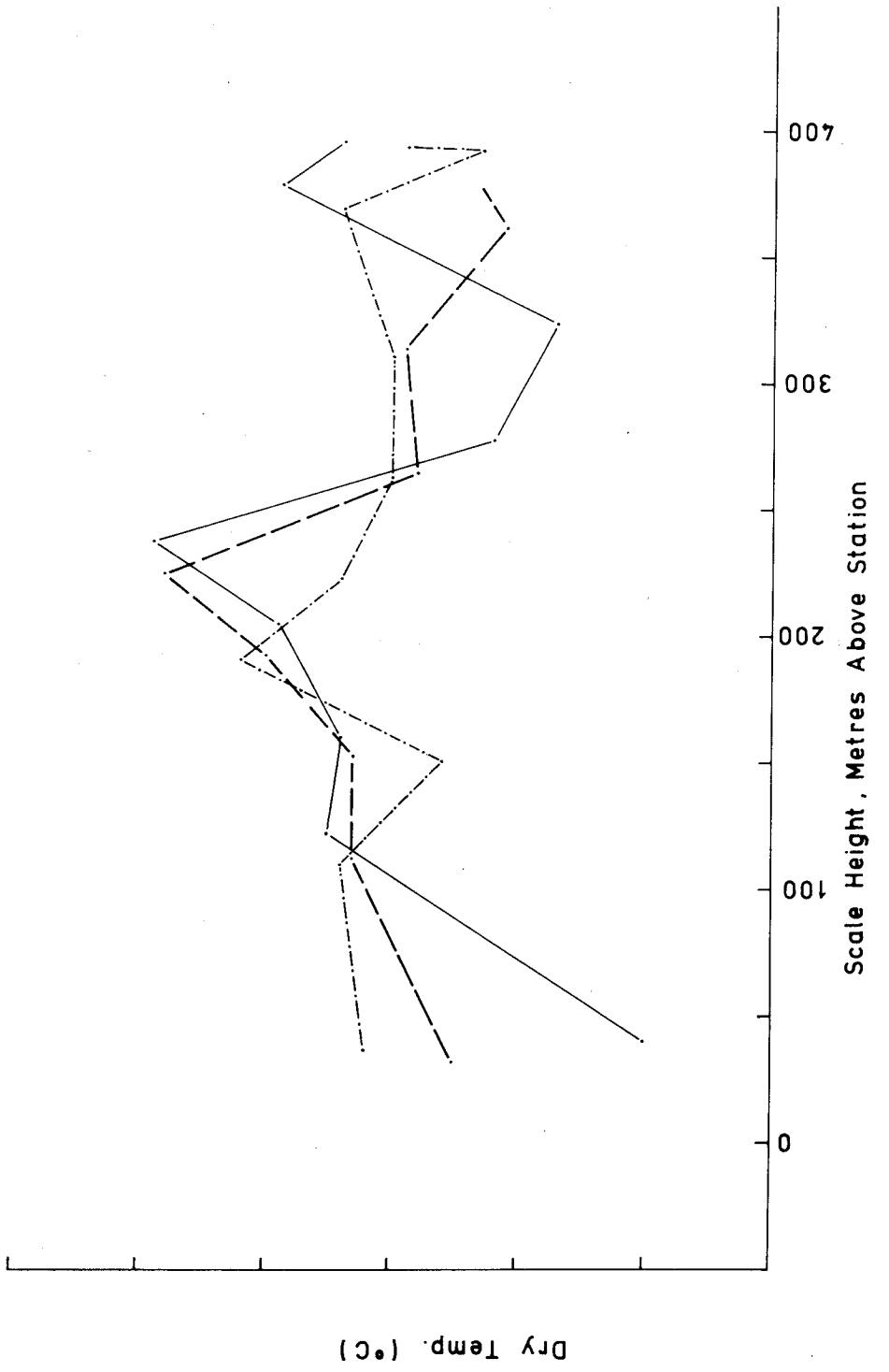

Figure 4. Temperature Profiles, Orroral Valley to Orroral Collimation Tower

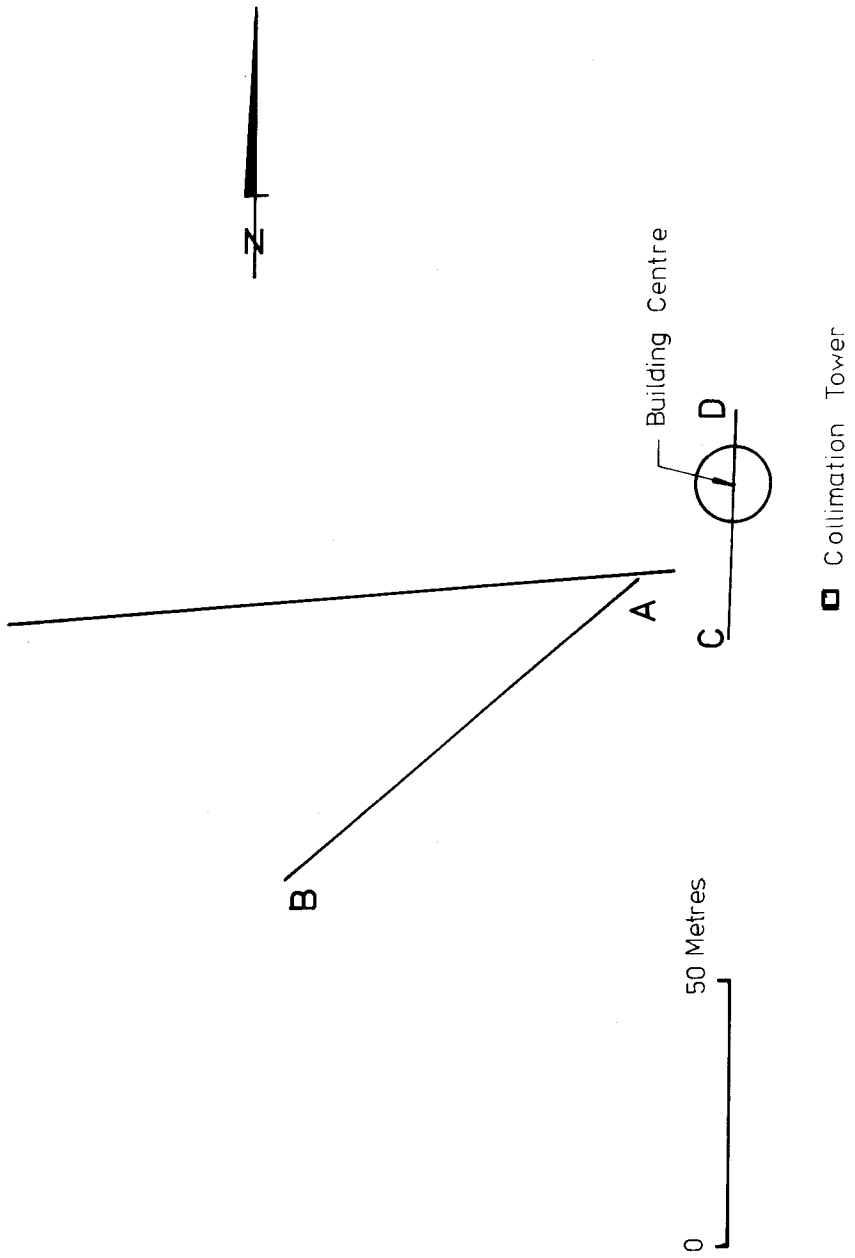

Figure 5. Plan of Seismic Geophone Arrays

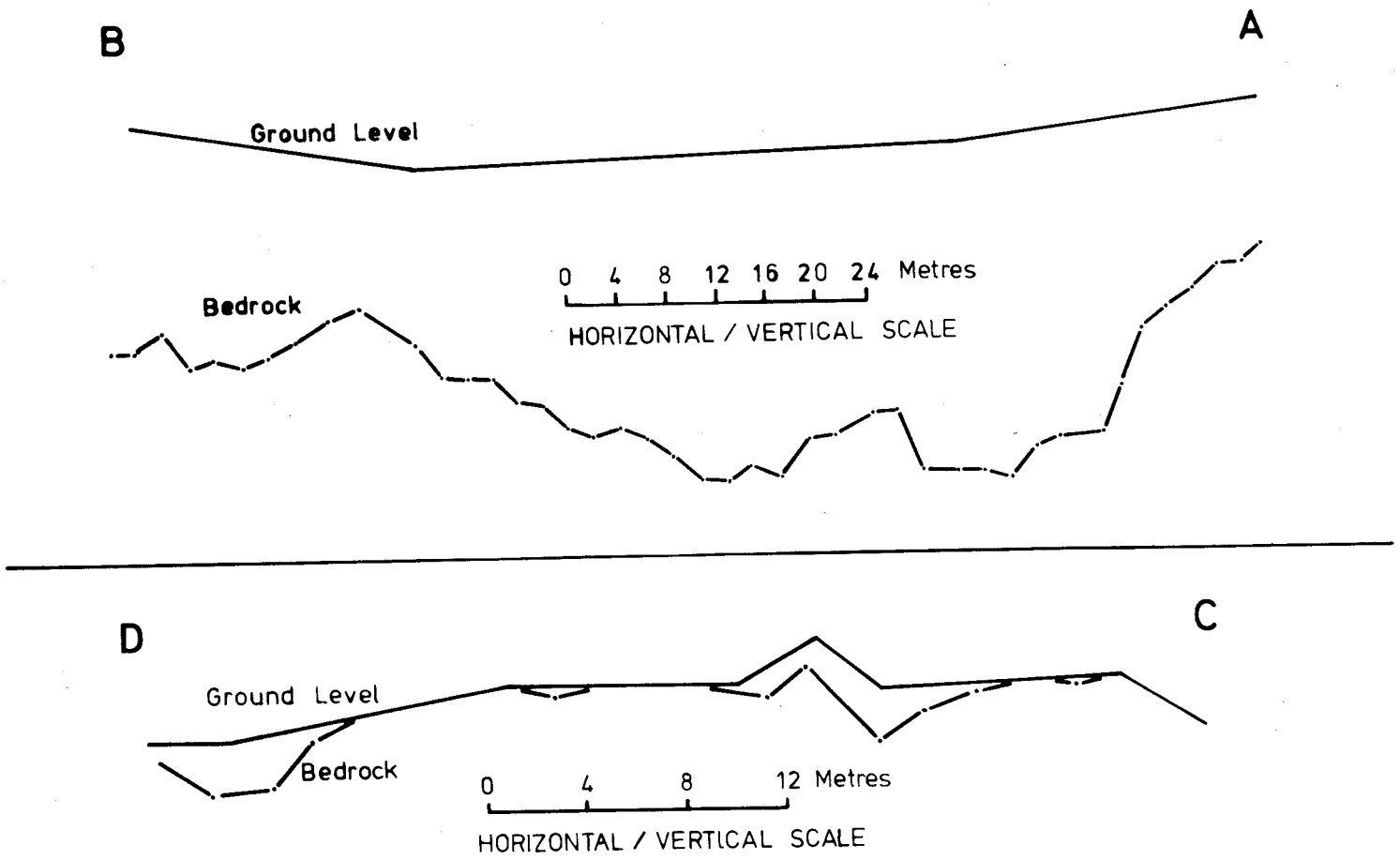

Figure 6. Bedrock Profile

2.7 Site Preparation

The current (November 1973) state of site preparation is that all necessary approvals have been obtained from the appropriate government departments, and that the area surrounding the selected rock has been cleared of those trees which would interfere with observations and access. The top of the rock has been cleared of weathered material preparatory to construction of the dome building for which tenders have been called. The 28'6" dome to surmount the brick structure has been ordered from the Ash-Dome company in the USA.

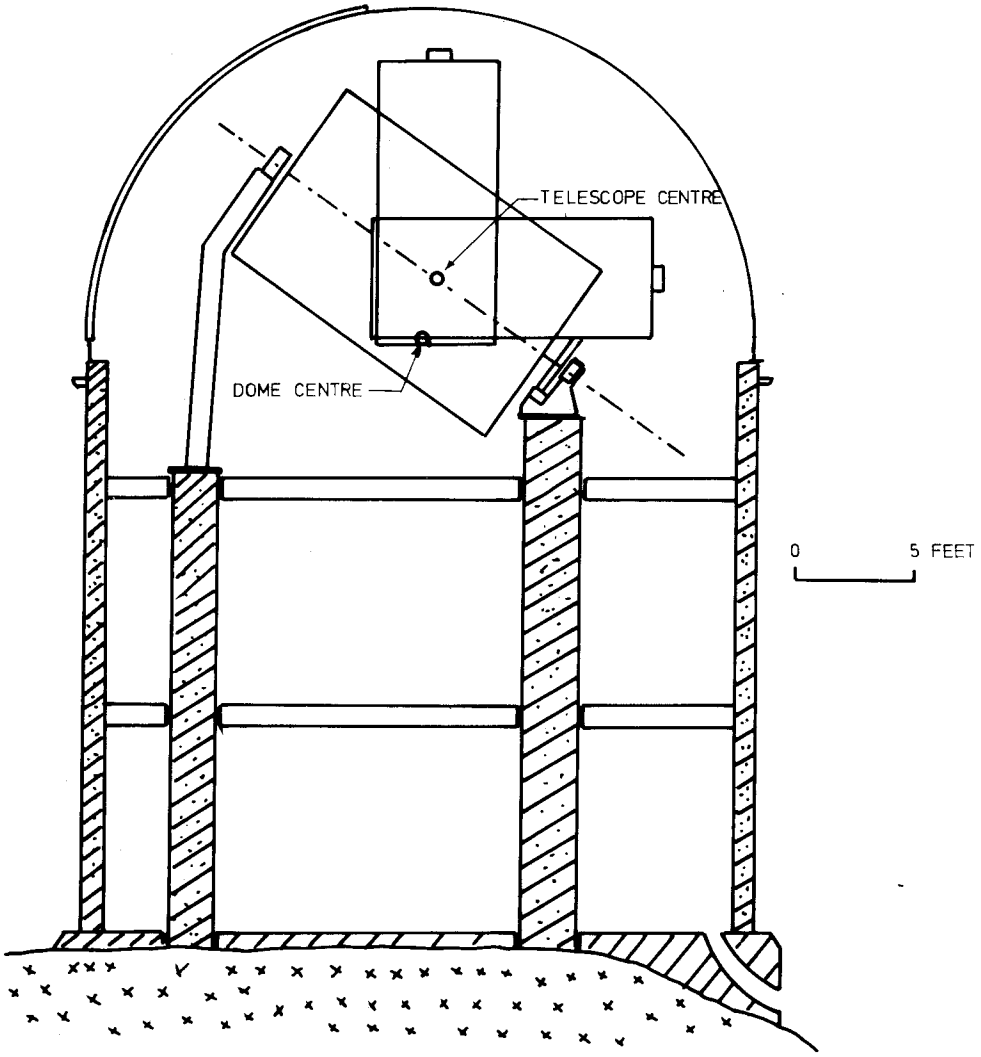

Figure 7. Lunar Ranger Building Cross Section

3. The Building

3.1 Construction

The building is to be a 28'6" external diameter double brick cylinder 25' high (LUCK et al in press) surmounted by a standard hemispherical Ash-Dome. The intersection of the telescope axes

will be 28'7" above the ground floor. There will be three floors - ground, intermediate and observation floors. Figures 7 and 8 show the layout of the building. The observation floor will contain the telescope, control console and laser pulse forming networks. The intermediate floor will be air-conditioned and will contain the control computer and its principal peripherals, the National Mapping clock ensemble, VLF receivers and associated electronic equipment, working space and room for the installation of control racks for future geodetic instruments. The ground floor will house loading bay, heavy power and air conditioning plant, toilet and meal table. The building will be constructed by contract from the Australian Department of Works.

3.2 Telescope Piers

The essential feature of the internal building is the set of three 18 inch piers to support the telescope legs. To ensure firmness and stability, they will be sunk four feet into the rock, and tied by 14 inch concrete beams just below each floor, including the ground floor. However, each pier will be mechanically isolated everywhere from the building by neoprene filled gaps so that no vibrations induced in the building by wind or other movement will be transmitted to the telescope.

4. The Telescope

4.1 Mounting

The telescope was built by Astro Mechanics Inc, Austin, Texas, to a minimum weight specification. It is supported at the south end by two vent legs whose feet are 15 feet apart, and at the north end by a pedestal containing the RA drive. Between them a strong rectangular frame carries two stub axles which form the declination axis and two stub axles forming the polar axis. The declination axles support the declination cube, a strong square box on which the laser box itself is mounted, and above and below which are mounted the Serrurier trusses which carry the spider of the secondary mirror, and the primary mirror. The telescope is to be assembled shortly in a workshop to check its operating condition prior to final reassembly.

4.2 Optics

BUCHROEDER et al (1972) have described the telescope optics. The essential features are shown in figure 9 and comprise an aluminised f2.5 152 cm CerVit primary slightly over-parabolised, a 40 cm gold coated hyperboloidal secondary which increases the effective focal ratio to f8, and a 23 cm x 15 cm elliptical, dichroic beamsplitter whose coating reflects 96% of light at 6943A^{o} but transmits most of the light 10A^{o} away. The beamsplitter, at 45^{o} to the optical axis, directs the laser beam to and from an aperture in the declination cube which gives optical access to the laser optical system.

The bulk of white light collected by the telescope passes through the dichroic beamsplitter and another 45^{o} glass plate situated in the centre hole of the primary in order to compensate coma and aberration introduced by the beamsplitter. This beam is then further split, part going to a visual eyepiece and part to the automatic tracker in the Cassegrain position. The eyepiece is placed on a graduated and calibrated X-Y stage so that the telescope can be set on a known lunar feature, such as a peak in a crater, then offset precisely to the position of the adjacent retroreflector array which is, of course, invisible but whose selenodetic coordinates are known. The offset can be computer calculated and, in the future, controlled.

The tracker consists of an ITT F4011 image dissector which is sufficiently sensitive to detect departures from the central position of features in full moon, daylight or possibly illuminated by

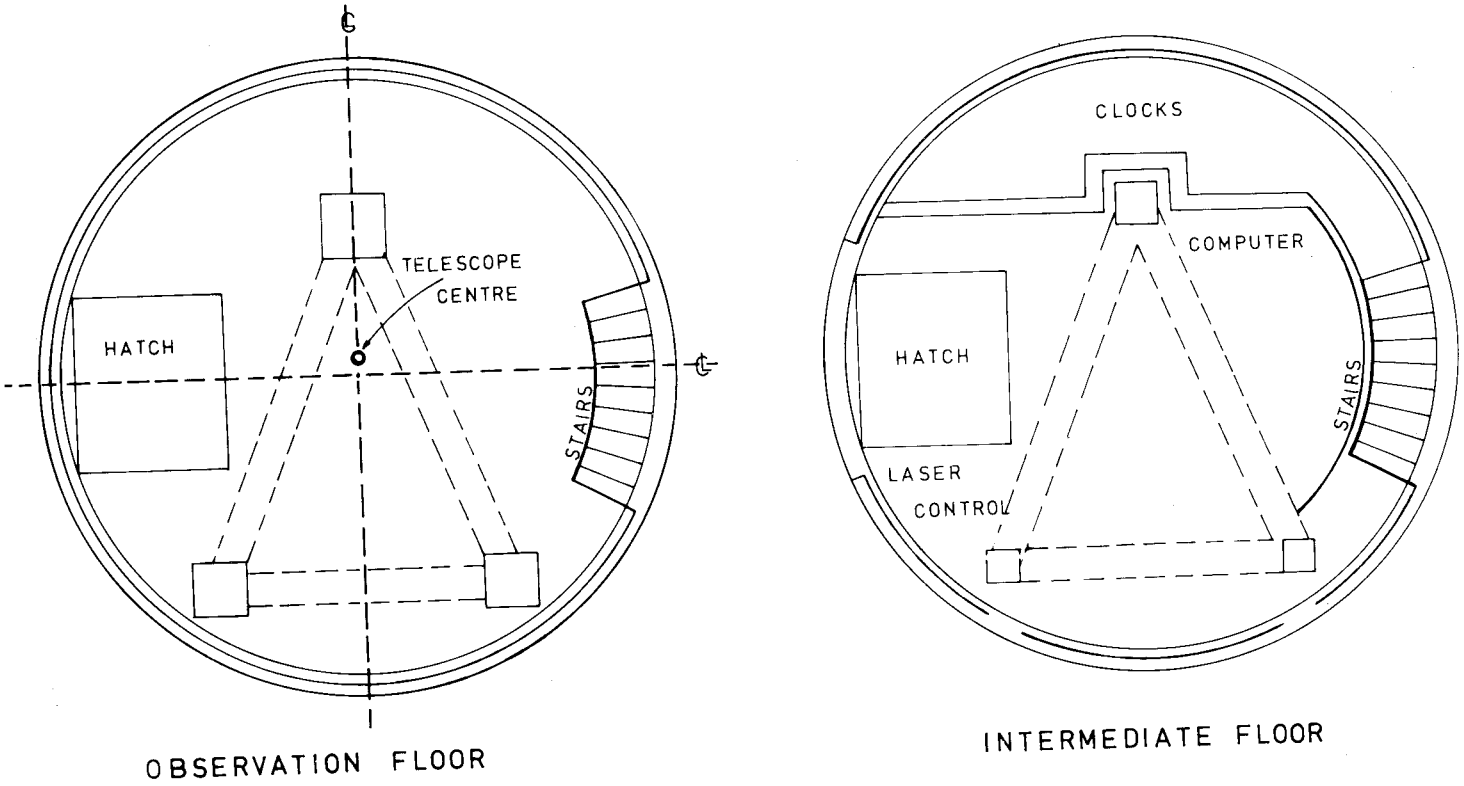

Figure 8. Lunar Ranger Building Floor Plans

earthshine. The correcting signals from the dissector tube drive stepping motors in 0.6 arcsecond steps in declination and hour angle to bring the feature back to centre position. This method of tracking obviates the need for a conventional clock or sidereal drive, and is equally suitable for tracking the moon, stars, or high altitude earth satellites.

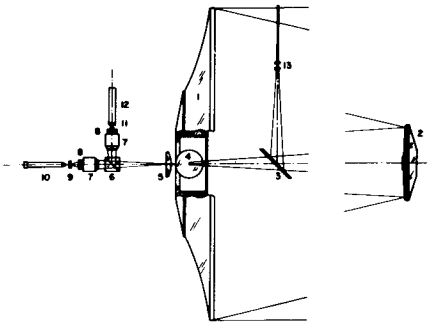

152-cm diam telescope. (1) 152-cm f/2.5 hyperboloid CER-VIT primary mirror. (2) 40-cm hyperboloid CER-VIT secondary mirror. (3) 23 X 15-cm elliptical dichroic beamsplitter (99% reflectivity at 694.3 nm). (4) 23 X 15-cm elliptical compensator plate. (5) 14-cm field lens. (6) 76-mm dichroic cube beamsplitter. (7) Nikkor-H 35-mm f/1.8 camera lens and portrait attachment. (8) Spherical aberration corrector plate. (9) Field flattener and reference reticle. (10) 40X microscope on X-Y stage. (11) Field flattener bonded to face of image dissector tube. (12) ITT F4011 image dissector tube. (13) Laser interfacing lenses.

Figure 9. Telescope Optics. (From BUCHROEDER et al 1972)

5. The Laser

5.1 Laser Generator

The laser was originally built by Hughes Aircraft. It consists basically (CARTER et al 1972) (see figure 10) of a mechanical Q-switched ruby laser oscillator to provide the initial pulse of 0.2 Joule in 17 nanoseconds, four cascaded ruby amplifier lasers each with gain 1.5, a Pockels cell to rapidly chop the pulse to 3 nanoseconds, turning prisms and mirrors to render the laser box reasonably compact, and a diverging lens matched to the telescope optical system and placed precisely at its focal point so that the beam emerging from the telescope is parallel to within 2 arcseconds. The laser has already been test fired in the Q-switched 17 ns pulse mode. Tests with another ruby laser revealed no radio interference to the tracking station antennae.

5.2 Receiver

The beam returns from the moon via a transmit-receive mirror through a tunable Etalon filter which permits only light of the ruby wavelength to reach the detecting photomultiplier tube whose output stops a time interval counter started approximately 2.5 seconds earlier by the outgoing pulse. The photomultiplier is sufficiently sensitive to detect a single return photon. That such a return photon comes from the original pulse rather than stray moonlight is ensured with high proba-

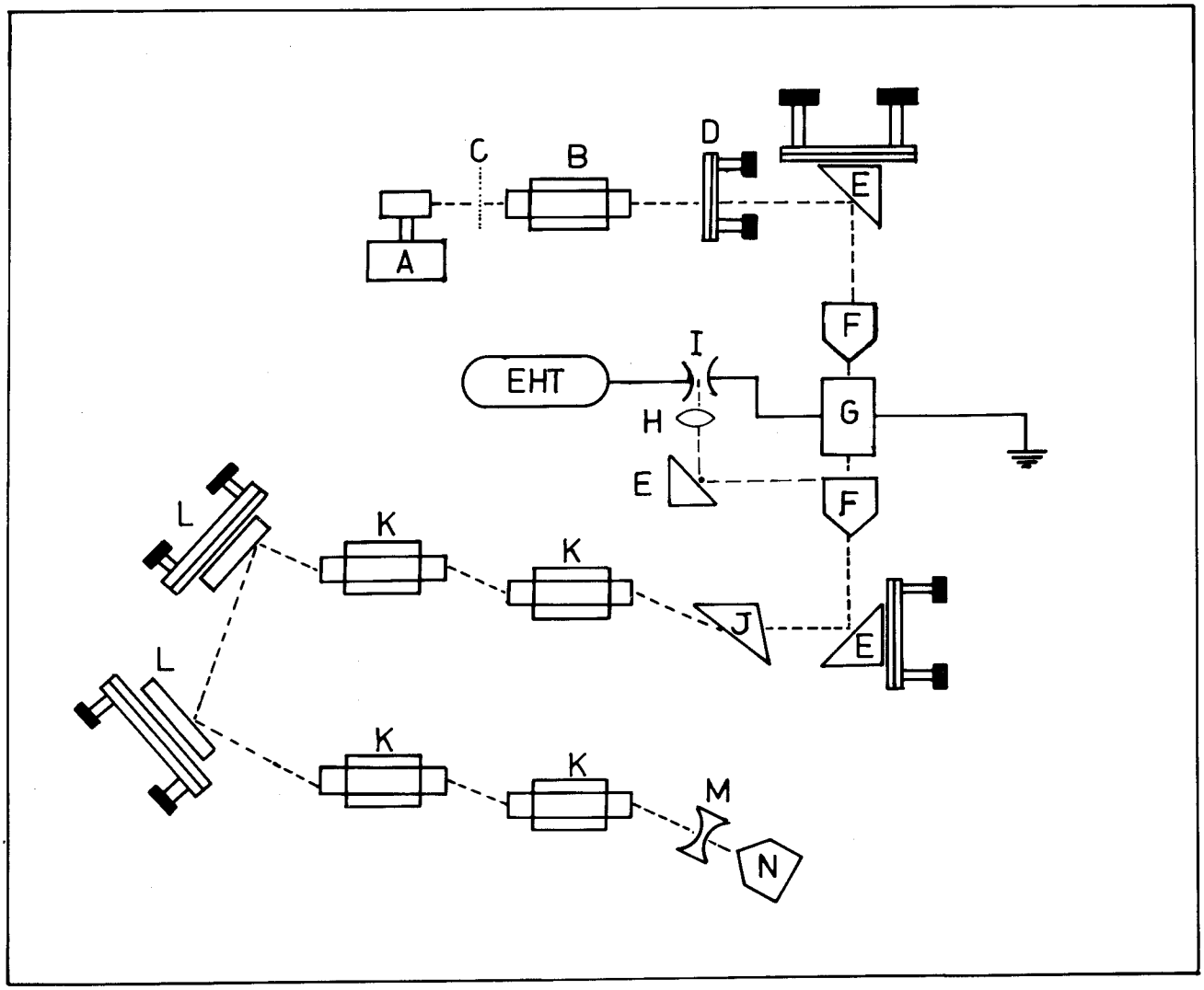

Figure 10. Laser box

(A) Rotating prism Q-switch. (B) Ruby laser. (C) Aperture stop.
(D) Sapphire mirror. (E) Turning prisms. (F) Glan polarising prisms.
(G) Pockels cell. (H) Focusser. (I) Spark gap. (J) Brewster prism.
(K) Ruby amplifiers. (L) Turning mirrors. (M) Diverging lens.
(N) Circulariser, turns beam to dichroic beamsplitter.

bility by three types of filtering: frequency filtering by the Etalon filter; spatial filtering by optical stops so placed that even errors in telescope collimation will impede the photon; and time filtering by gating the photomultiplier with a window one or two microseconds wide about the expected return time.

The single photon sensitivity of the receiver is required since the original 150 cm beam has expanded, assuming 2 arcsecond divergence, to a diameter of 4 km at the moon, whereas only 1/3 square metre is returned by the retroreflector array, that is only one part in 4×10^7 is returned. A similar attenuation occurs between the moon and earth on the homeward journey. The atmosphere absorbs a considerable proportion of the energy in each direction, as do the numerous optical surfaces in the laser, telescope and receiver.

5.3 Shot Sequence

The laser firing sequence is controlled by an on-line computer, which also computes and sets the range gate by means of Chebyshev polynomials interpolating the lunar ephemeris initially to be provided by the Jet Propulsion Laboratory, Pasadena, California. The firing sequence will initially be 200 shots at 5 second intervals, repeated to each of the available lunar retroreflectors, particularly the American ones at Hadley's Rille, Fra Mauro and Mare Tranquillitatis. It is hoped eventually to reduce the interval between shots to the limit of 3 seconds required for the capacitor banks of the pulse forming networks to recharge between shots.

6. RANGE EQUATIONS

FAJEMIROKUN (1971), KAULA (1973) and MUELLER et al (1972) have described the range equations and analysed them numerically from different standpoints for various needs. A brief description follows, together with suggestions for obtaining the sidereal time, polar motion components and continental drift explicitly from the adjustment solutions, these quantities being of particular interest to the Division which is very well placed to compare these quantities determined by the LLR against determinations by its PZT.

6.1 Topocentric Coordinates of a Retroreflector

The distances will be expressed eventually in terms of X, Y, Z components in the very nearly inertial geocentric ecliptic coordinate system at epoch 1950.0, say. Conventional rotation matrices (MUELLER 1969) $R_1(\alpha)$, $R_2(\beta)$, $R_3(\gamma)$, denoting rotations of α,β,γ about the X,Y,Z axes respectively,,and Lucas matrices L_1, L_2, L_3 such that

$$\frac{\partial R_1(\alpha)}{\partial \alpha} = L_1 R_1(\alpha)$$

will be employed throughout.

Let $[U,V,W]^T$ be cartesian coordinates in a geodetic system of the laser station T, and let $[X_p,Y_p,Z_p]^T$ be its coordinates in the 1950.0 ecliptic system. Then

$$\begin{bmatrix} U \\ V \\ W \end{bmatrix} = \begin{bmatrix} (N + h) \cos \phi \cos \lambda \\ (N + h) \cos \phi \sin \lambda \\ [N(1-e^2) + h] \sin \phi \end{bmatrix} \qquad (1)$$

in standard notation.

If ε_o is the obliquity of the ecliptic 1950.0, z_1, θ_1 and ζ_o are precession parameters (HMSO 1961), ε, $\Delta\varepsilon$ and $\Delta\psi$ are nutation parameters, x_p and y_p are the instantaneous coordinates of the pole relative to the CIO of 1903.0 and S is the current sidereal time, then

$$\begin{bmatrix} X_p \\ Y_p \\ Z_p \end{bmatrix} = R_1(\varepsilon_0)R_3(\zeta_0)R_2(-\theta_1)R_3(z_1)R_1(-\varepsilon)R_3(\Delta\psi)R_1(\varepsilon+\Delta\varepsilon)R_3(-S)R_1(y_p)R_2(x_p)\begin{bmatrix} U \\ V \\ W \end{bmatrix} . \qquad (2)$$

Similarly, if ψ,θ,Φ, are the Euler angles of the orientation of the selenodetic coordinate system, and $[x_m,y_m,z_m]^T$ are the coordinates of the retroreflector R in the selenodetic system, its coordinates $[X_m, Y_m, Z_m]^T$ in the 1950.0 ecliptic system will be

$$\begin{bmatrix} X_m \\ Y_m \\ Z_m \end{bmatrix} = R_1(\varepsilon_0)R_3(\zeta_0)R_2(-\theta_1)R_3(z_1)R_1(-\varepsilon)R_3(-\psi)R_1(\theta)R_3(\Phi)\begin{bmatrix} x_m \\ y_m \\ z_m \end{bmatrix} . \qquad (3)$$

The geocentric 1950.0 equatorial coordinates of the lunar centre M, $[X_{cq},Y_{cq},Z_{cq}]^T$ are obtained from a lunar ephemeris and transformed to the 1950.0 ecliptic system by

$$\begin{bmatrix} X_c \\ Y_c \\ Z_c \end{bmatrix} = R_1(\varepsilon_0)\begin{bmatrix} X_{cq} \\ Y_{cq} \\ Z_{cq} \end{bmatrix} . \qquad (4)$$

Reference to figure 1 then shows that the coordinates $[X_{m_t}, Y_{m_t}, Z_{m_t}]^T$ of the retroreflector relative to the telescope are

$$\begin{bmatrix} X_{m_t} \\ Y_{m_t} \\ Z_{m_t} \end{bmatrix} = \begin{bmatrix} X_c \\ Y_c \\ Z_c \end{bmatrix} + \begin{bmatrix} X_m \\ Y_m \\ Z_m \end{bmatrix} - \begin{bmatrix} X_p \\ Y_p \\ Z_p \end{bmatrix} . \qquad (5)$$

The measured distance d obtained by lunar laser ranging is

$$d = (X_{m_t}^2 + Y_{m_t}^2 + Z_{m_t}^2)^{\frac{1}{2}} .$$

6.2 Observation Equations

The design matrix A of the observation equations in the adjustment is (CARTER et al 1972)

$$A = \frac{\partial D}{\partial x} = \frac{\partial D}{\partial X_t} \cdot \frac{\partial X_t}{\partial x} \qquad (6)$$

where D is the column vector of parametrised distances d_i,

$$X_t = [X_{m_t}, Y_{m_t}, Z_{m_t}]^T,$$

and X is the column vector of all the parameters.

The partial derivatives of particular interest are those concerned with sidereal time, polar motion and continental drift.

6.2.1 Sidereal Time and Polar Motion

The sidereal time S can be modelled as

$$S = UTC + B^t T + \Delta\psi \cos\varepsilon + S_1 \tag{7}$$

where UTC is a uniform time scale, $B^t T$ is the usual conversion in terms of t, the number of Julian centuries elapsed since 1900 Jan 0.5UT, $\Delta\psi \cos\varepsilon$ is the equation of the equinoxes and S_1 is a model of the variation in the rate of rotation of the earth:

$$\begin{aligned} S_1 = {} & s_1 \cos(2\pi.36525t) + s_2 \sin(2\pi.36525t) \\ & + s_3 \cos(2\pi.100t) + s_4 \sin(2\pi.100t) \\ & + s_5 \cos(2\pi.86t) + s_6 \sin(2\pi.86t) \end{aligned} \tag{8}$$

The first two terms of S_1 represent the diurnal variation which may be better determined by laser ranging than by Photographic Zenith Tubes, since observations can cover all hours of the day in the course of the month, while the other terms represent annual and Chandler variations. The expression for the partial derivative in s_1 is

$$\frac{\partial X_t}{\partial s_1} = \frac{\partial X_t}{\partial S} \cdot \frac{\partial S}{\partial s_1} = R_1(\varepsilon_0) P^t N^t L_3 R_3(-S) R_1(y_p) R_2(x_p) \begin{bmatrix} U \\ V \\ W \end{bmatrix} \cos(2\pi.365252t)$$

where P^t is written for the precession matrices and N^t for the nutation matrices. Similar expressions hold for the other coefficients. Again, the polar motion terms x_p and y_p can be similarly modelled in terms of diurnal, annual and Chandler periods.

6.2.2 Continental Drift

The simplest model of continental drift relative to an absolute geodetic datum is to let

$$\begin{bmatrix} U \\ V \\ W \end{bmatrix} = \begin{bmatrix} U_o + ut \\ V_o + vt \\ W_o + wt \end{bmatrix}$$

from which is obtained representatively

$$\frac{\partial X_t}{\partial u} = -R_1(\varepsilon_0) P^t N^t R_3(-S) R_1(y_p) R_2(x_p) \begin{bmatrix} t \\ o \\ o \end{bmatrix} \tag{10}$$

These proposals are currently conjectural. Numerical experiments by KAULA suggest that station drift parameters, especially in the east-west direction, will be well determined although, naturally, highly correlated with station location, and that sidereal time and polar motion parameters should include monthly and bimonthly terms as well.

7. Acknowledgment

The authors wish to thank the Canberra Bureau of Meteorology for providing data and assistance; the Bureau of Mineral Resources for conducting the geophysical surveys; and staff of the Australian National University for advice on siting and building. The Director of the Weapons Research Establishment, South Australia, kindly made available a pulsed ruby laser for radio interference tests. They are grateful to Mr R. CAMERON for the loan of his eight inch telescope. They thank the Director of the STDN facility at Orroral Valley for his good offices, and finally, the officers of the Division of National Mapping who have contributed towards this project.

8. References

BUCHROEDER, R.A., ELMORE, L.H., SHACK, R.V. & SLATER, P.N. 1972. *The Design, Construction and Testing of the Optics for a 147-cm Aperture Telescope.* Final Report for AFCRL, Bedford, Mass. USA. Contract F19628-72-C-0047.

CARTER, W.E., ECKHARDT, D.H. & ROBINSON, W.G. 1972. *AFCRL Lunar Laser Instrumentation Status Report.* AFCRL Report 72-0615.

FAJEMIROKUN, F.A. 1971. *Applications of Laser Ranging and VLBI Observations for Selenodetic Control.* Report No.157, Department of Geodetic Science, Ohio State University, for NASA Manned Spacecraft Centre, Houston, Texas, USA. Contract NAS (9-9695 1971)

HMSO. 1971. *Explanatory Supplement to the Astronomical Ephemeris.*

HYLAND, A.R. 1973. Private Communication.

KAULA, W.M. 1973. *Phil.Trans.Roy.Soc. Lond. A* 274,185-193.

KIEPENHEUER, K.O. 1962. "Le Choix des Sites d'Observatoires Astronomiques" in ROSCH, J.(ed) *IAU Symposium No.*19.

LUCK, J. McK., MILLER, M.J. & MORGAN, P.J. *Proc.Astron.Soc. of Australia.* In Press.

MEINEL, A.B. 1963. "Astronomical Seeing and Observatory Site Selection" in KUIPER, G.P. & MIDDLEHURST, B.M. (eds). *Telescopes.* 158.

MUELLER, I.I., FAJEMIROKUN, R.A. & PAPO, H.B. 1972. *Report to Annual Meeting of COSPAR.* Madrid

MUELLER, I.I. 1969. *Spherical and Practical Astronomy as applied to Geodesy.* Frederick Ungar Publishing Co. New York.

REITAN, D. 1963.*J. App. Meteorology.* 2, 776.

9. Discussion

PLOTKIN: We hear something of the difficulties involved. We are using beams which are 2 - 3 arcsec in diameter and most astronomical telescopes while they can guide accurately, cannot point absolutely in that sense. The Hawaiian station is one of the few attempts to do absolute pointing with an instrument that large.

MORGAN†: Whether or not this will increase the nights per lunation on which data can be acquired is still not certain.

† Post-symposium comment.

CARTER, W. E.
WILLIAMS, J. D.
Institute for Astronomy
University of Hawaii
Hawaii

Proc.Symposium on Earth's Gravitational Field & Secular Variations in Position (1973),433-441.

UNIVERSITY OF HAWAII LURE OBSERVATORY

ABSTRACT

The University of Hawaii Institute for Astronomy is constructing a lunar laser ranging observatory at the summit of Mt. Haleakala, Maui, Hawaii. The project is funded by the National Aeronautics and Space Administration and the design, construction, and operation of the station are being closely coordinated with the LURE Team.

Instrumentation has been developed at the University of Maryland, Wesleyan University, JILA National Bureau of Standards and the University of Colorado, University of Texas, University of Hawaii, and NASA Goddard Space Center.

The laser is frequency doubled Nd YAG operating at three pulses per second; each pulse is 200 picoseconds (FWHM) in duration, and contains 250 millijoules of energy at 5320 Å.

The laser is coupled into a 40 cm aperture refractor telescope. The telescope expands and collimates the laser pulses, and directs them toward a 68 cm diameter altitude-azimuth mounted flat mirror referred to as a lunastat. The lunastat is positioned so that the reflected beam is pointed at the desired target by fully automatic, computer controlled absolute pointing or by offset guiding techniques.

The return signal is received by a multi-lensed telescope referred to as the lurescope. The light collected by eighty 19 cm aperture achromatic lenses is routed to a common focus, spatially and optically filtered, beamsplit, and detected by two photomultiplier tubes. The output of each PMT is connected to one channel of a dual channel multi-event timer system.

The event timer determines the epoch of each start and stop event, on the station timescale, with a resolution of 100 picoseconds. The total uncertainty of each range measurement is approximately 500 to 600 picoseconds. An observation consists of several range measurements.

Two mini-computers are used to generate range predictions, retrieve and store range data, control the telescope drive, read and store meteorological data, and perform numerous other housekeeping duties.

Current planning anticipates ranging to begin in mid 1974.

1. Introduction

The University of Hawaii's Institute for Astronomy is currently constructing a lunar laser ranging observatory at the 3050-meter summit of Mt. Haleakala, Maui, Hawaii. The project is funded by NASA under contract NASW-2326, with J. T. Jefferies as Principal Investigator. The design, construction, and operation of the station is being closely coordinated with the LURE team and many of the major components of the system are being built by D. CURRIE ET AL at the Department of Physics and Astronomy, University of Maryland; J. FALLER ET AL at Wesleyan University and the Joint Institute for Laboratory Astrophysics, National Bureau of Standards and the University of Colorado; and by H. PLOTKIN ET AL, NASA Goddard Space Center, Maryland.

2. The Observatory

Figure 1 is a cutaway east elevation of the University of Hawaii LURE Observatory.

At the north end of the observatory a 9-meter diameter dome (Ash Dome Inc.) houses the receive telescope (Lurescope). The Lurescope dome is connected to the main building by an enclosed hallway.

The main building, containing the control and timing electronics, the laser and transmitter system, and support facilities, is a 9 x 19 - m prefabricated steel structure. A 0.5-meter crawl space beneath the raised working level accommodates the air conditioning, electrical distribution and sanitary systems. An articulated light path used to route a portion of the laser light to the Lurescope for the purposes of tuning the narrow bandpass filer and calibrating the timing system, is also located in the crawl space.

The transmitter system is located near the south end of the observatory and is constructed on two levels. The lower level is a laboratory environment that houses the laser and interfacing optics, the lunastat drive and pointing electronics, and the pointing optomechanical instrumentation. The upper level, reached by stairway from the laboratory area, is enclosed in a 7-meter diameter dome (Ash Dome Inc.) and contains the primary optics of the refractor feed telescope and the lunastat. The isolated instrument pier extends from beneath the laboratory level to the upper level. All the optomechanical components of the transmitter system, including the laser, interfacing optics, pointing instrumentation, feed telescope, and lunastat are mounted on this common pier.

3. The Laser

The Nd YAG laser system (figure 2), developed by GTE Sylvania, Electronic Systems Group of Mountain View, California, under a NASA Goddard Space Center contract, provides three pulses per second, each pulse being approximately 200 picoseconds in duration (FWHM) and containing 250 millijoules of energy at 5320 Å.

The basic elements of the system are: a mode locked oscillator, a regenerative amplifier, three single pass amplifiers, and a CsD*A (caesium dideuterium arsenate) frequency doubling crystal.

The oscillator cavity is formed by two reflectors spaced at approximately 1 meter and supported on isolation-mounted Invar rods. The oscillator head contains a 3.8-mm diameter by 70-mm rod, pumped continuously by two tungsten-halogen incandescent lamps. Mode locking is accomplished by a Data Light Inc. acousto-optic mode locker operated at 75 MHz. The output of the oscillator is a 150 MHz train of 200 picosecond duration pulses each containing approximately 2 nanojoules of energy at 10 640 Å.

Upon command, a pair of pockels cells switch a single pulse out of the train and inject it into the regenerative amplifier. After 12 passes of the pulse through the regenerative amplifier, which utilizes a 6-mm diameter by 76-mm rod apertured to 3 mm, the pulse is switched out, expanded and routed to the single pass amplifiers. The pulse passes through two 6-mm diameter by 76-mm amplifiers, is further expanded and passes through a 9.5-mm diameter by 76- millimetre saturated amplifier. The 200 picosecond pulse then contains approximately 500 millijoules of energy at 10 640 Å and has a beam divergence of approximately three times the diffraction limit.

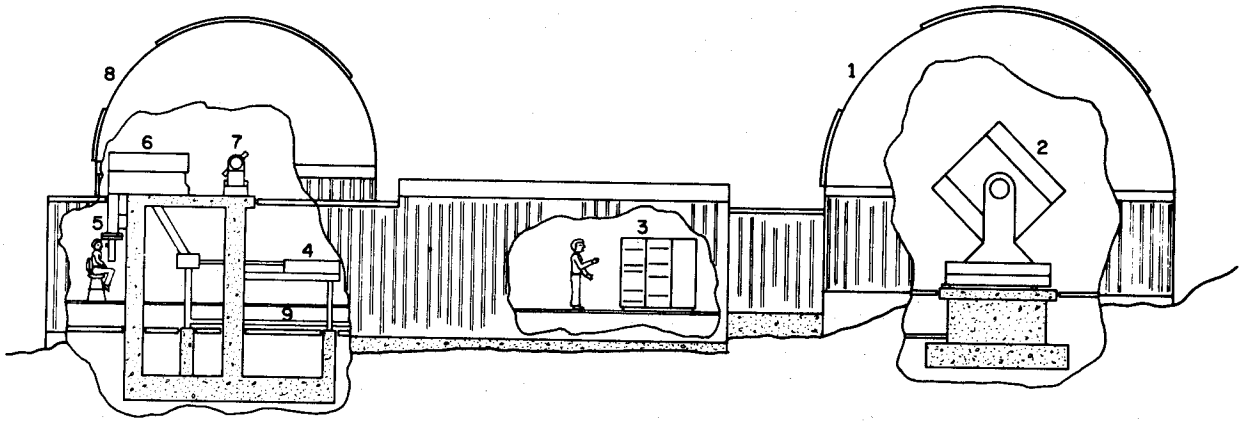

Figure 1. University of Hawaii LURE Observatory

1. 9-Meter Diameter Dome
2. Lurescope
3. Control & Timing Electronics
4. Laser
5. Pointing Instrumentation
6. Feed Telescope
7. Lunastat
8. 7-Meter Diameter Dome
9. Calibration Light-Link

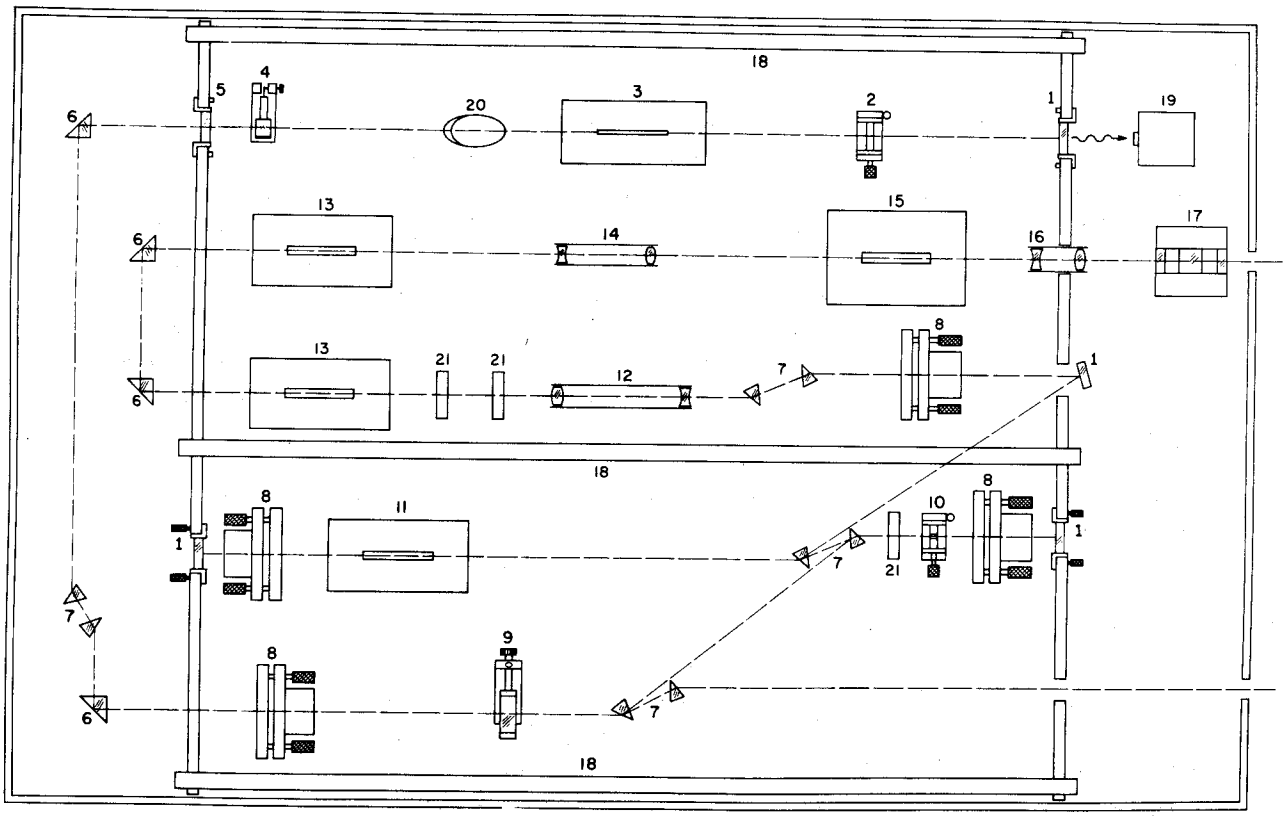

Figure 2. Laser

1. 99.9% Mirror
2. Aperture
3. Oscillator Head (3.8 x 70 mm rod)
4. Acousto-Optical Modulator
5. 98% Mirror
6. Turning Prism
7. Calcite Prisms
8. Pockels Cell
9. Beam Height Adjustment
10. Aperture
11. Regenerative Amplifier (6 x 76 mm rod)
12. Beam Expander Telescope
13. Single-Pass Amplifier (6 x 76 mm rod)
14. Beam Expander Telescope
15. Single-Pass Amplifier (9.5 x 76 mm rod)
16. Beam Expander Telescope
17. CsD*A Doubling Crystal
18. Invar Mounting Rods
19. Photo-detector
20. Brewster Plate
21. $\lambda/4$ Plate

The infrared is frequency-doubled by a CsD*A crystal to produce the desired 5320 Å light. The doubling crystal further deteriorates the beam collimation to 6 - 8 times the diffraction limit. Residual infrared is stripped-off by reflection from two dichroic mirrors prior to coupling into the transmitter system.

4. The Transmitter

Figure 3 is a sketch of the laser transmitter system (CARTER 1973). The collimated laser light is routed to a diverging lens. The diverging lens creates a diverging cone of light that appears to emanate from a point lying in the focal plane of the telescope objective. The diverging light is routed by reflection from a dichroic beamsplitter to the 40-cm diameter objective. The objective recollimates the expanded beam and transmits it toward the Lunastat. The reflected beam is pointed by accurate positioning of the lunastat and exits the enclosing observatory dome through a window of 75 cm diameter. A portion of the transmitted beam is intercepted by a cube corner and retroreflected. Approximately 0.2% of the reflected light passes through the dichroic beamsplitter and is routed to the pointing ocular which is mounted on a precise X-Y stage. The entire system, including the laser, is mounted on a common rigid frame concrete instrument pier.

5. The Lunastat

The Lunastat was constructed by Goerz-Inland Systems Division, Kollmorgen Corporation of Pittsburgh, Pennsylvania. A 70 cm diameter ultra-lightweight (25 kg) fused quartz optical flat, loaned for the duration of the project by the Optical Sciences Center, The University of Arizona, is the principal optical component. The mounting is altitude-azimuth; stabilized castings and maximum symmetry on construction have been used to minimize structural flexure and temperature related distortions of the mount. The design incorporates previously developed units consisting of mechanical axis, direct coupled torque motor drive, d.c. tachometer, and Inductosyn electronic shaft encoder. The axis wobble is <2.0 arcseconds; the encoder has a resolution of 0.36 arcsecond. The electronic logic, control, and readout units are standard production items. Both manual and computer control modes are available.

A two axis electronic level has been built into the instrument to provide a real time measurement of tilt, and appropriate corrections are made in formulations of the pointing commands.

6. Feed Telescope

The principal imagery element of the feed telescope is the 40 cm diameter f/11 achromatic objective. The two elements of the objective are widely airspaced ($\sim$ 20 cm) for the purpose of eliminating spherochromatism. The objective is diffraction-limited, monochromatically, over the visible spectrum, and image splitting by wavelength selection allows the objective to be used simultaneously for three distinct purposes: transmitting laser pulses, visual viewing, and electronic viewing.

The laser transmitting path and the two viewing optical paths are interfaced to the objective by use of a 2.5 cm thick, 33 cm diameter fused quartz beamsplitter located approximately 152 cm from the objective. The beamsplitter is dielectric coated to have >99.5% reflection at the laser wavelength of 5320 Å region. Light passing through the beamsplitter does suffer significant optical aberrations; an array of three optically flat corrector plates is used to compensate these

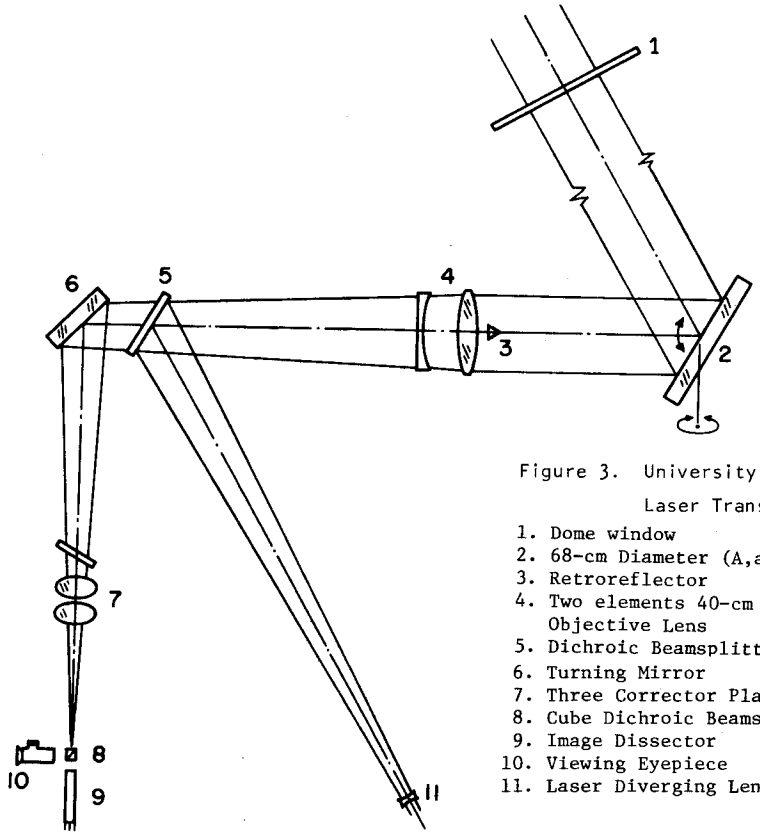

Figure 3. University of Hawaii Laser Transmitter System

1. Dome window
2. 68-cm Diameter (A,a) Mounted Flat
3. Retroreflector
4. Two elements 40-cm Diameter Objective Lens
5. Dichroic Beamsplitter
6. Turning Mirror
7. Three Corrector Plates
8. Cube Dichroic Beamsplitter
9. Image Dissector
10. Viewing Eyepiece
11. Laser Diverging Lens

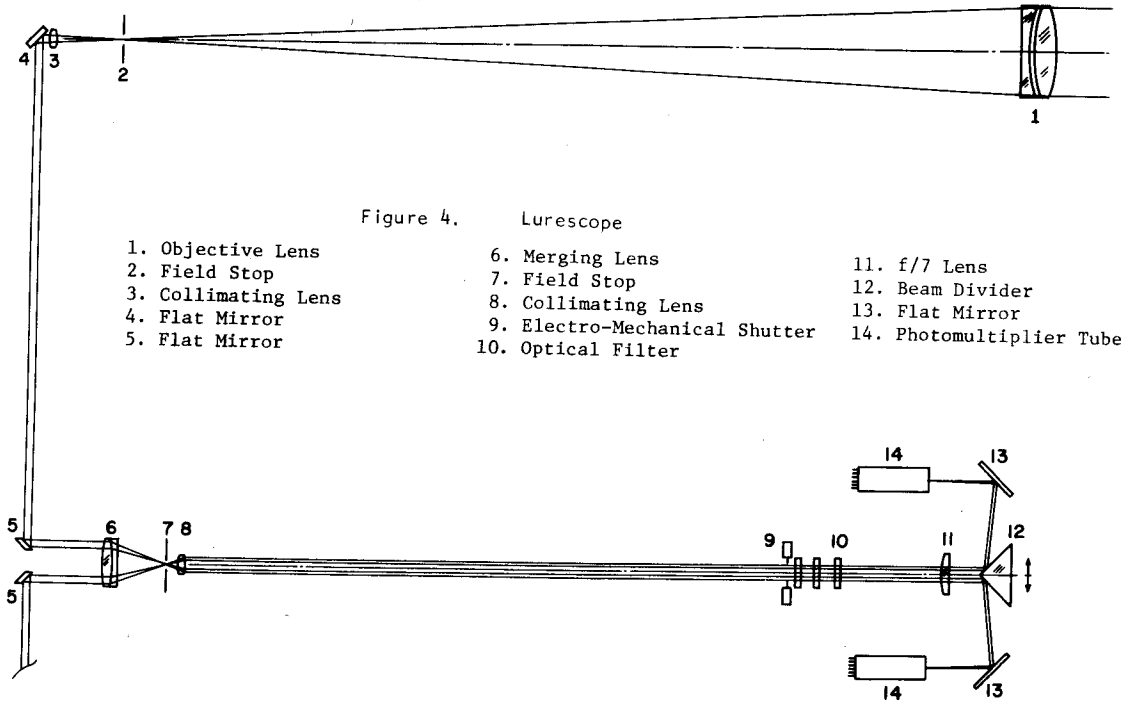

Figure 4. Lurescope

1. Objective Lens
2. Field Stop
3. Collimating Lens
4. Flat Mirror
5. Flat Mirror
6. Merging Lens
7. Field Stop
8. Collimating Lens
9. Electro-Mechanical Shutter
10. Optical Filter
11. f/7 Lens
12. Beam Divider
13. Flat Mirror
14. Photomultiplier Tube

aberrations. This light is further subdivided, by use of a cube dichroic beamsplitter, and routed to an ocular and image dissector tube mounted on the X-Y stage.

The feed telescope body and optical mounts were constructed by the University of Hawaii, in-house. The optical components were fabricated by Hudson Precision Optical Co., Inc. of Hudson, New Hampshire.

The feed telescope optics were designed by R.A. Buchroeder.

7. Relative Pointing System

The feed telescope, described above, has a nominal focal plane scale of 48 arsec/mm, resulting in a lunar image approximately 3.8 cm in diameter. A precise X-Y positioning stage, Yosemite Laboratory of Berkeley, California, is attached rigidly to the telescope tube and carries an assembly containing both an observer eyepiece and an image dissector tube, ITT F4012 RP. The stage is driven by stepping motors, Superior Electric Inc. type LS50-1006, having 500 steps per rotation. Each full rotation of the motors translates the stage 0.254 cm, making a single step equal to approximately 0.22 arcseconds. Maximum deviation from linearity over the entire 10-cm travel, each axis, is 0.0020 mm. Orthogonality of the axes is better than 10 arcseconds and flatness to travel is better than 0.0020 mm over the entire travel. Total positioning uncertainty over the full 10-cm x 10-cm field is less than 0.25 arcseconds. Temperature effects, about 1 part in 10^5 per degree centigrade, are insignificant over a range $\pm 3^{o}$C expected for the observatory ambient temperature.

Positioning of the stage may be controlled from a manual control panel or by computer command. A one-pulse-per-rotation shaft encoder is mounted on each drive motor. The total number of steps is recorded and the position is inferred directly. Whole numbers of rotations are checked for coincidence with the encoder pulse as a check against loss or addition of spurious counts. The laser will be aligned to the center of the stage travel as nearly as conveniently possible, and the actual coordinates will serve as fiducial. Offsets thus will be measured relative to the laser coordinates. Star fields and lunar features will be used to calibrate the focal plane distortions.

Use of two modes of relative pointing is anticipated. The modes differ, however, only in the means used to generate the basic lunar rate, i.e., by computer control or electronic tracker control of the Lunastat. The first method uses absolute methods continually to update the pointing, and the observer is required only to apply small corrections as required for deficiencies in the computer modelling. It is the ultimate goal that computer pointing be developed to the level of accuracy that the observer may be eliminated from the system and truly absolute pointing methods used.

The second method uses an image dissector tube as a sensor to lock onto and track a reference lunar feature. The observer still must make small pointing corrections as the offset changes with time. Comparison of electronic tracking and computer pointing will be used to improve the absolute point program model.

8. The Receiver (Lurescope)

FALLER's group built the receiver referred to as the Lurescope (FALLER 1972). The Lurescope consists of a "bundle" of 19-cm aperture refractor telescopes that are optically coupled to form a single image.

For the laser ranging a second field stop is placed in the common focal plane. The light passing through this spatial filter is collimated, routed through an optical filter, (typically, 2 to 3 Å) beamsplit, and routed to two photomultiplier tubes. Figure 4 is a schematic of the optical elements of a typical channel.

The Lurescope has an altitude-azimuth mount. The vertical axis has oil bearings; the horizontal axis has mechanical bearings. The drives are torque motors coupled to the axes by metal rollers. Twenty-bit, 1.2 arcsecond, optical shaft encoders measure the rotations about each axis. The primary method of pointing is absolute, under the control of Data General Corporation Super Nova Computer. A guide telescope is provided for manual guiding and/or for the observer to "touch-up" the computer pointing.

9. University of Maryland Event Timer System

Currie's group developed a clock system that is capable of measuring the epoch of individual events with a resolution of 100 picoseconds and, by differencing, determine the interval between two events occurring within a few seconds of one another to approximately 200 picoseconds. Figure 5 is block diagram of the system.

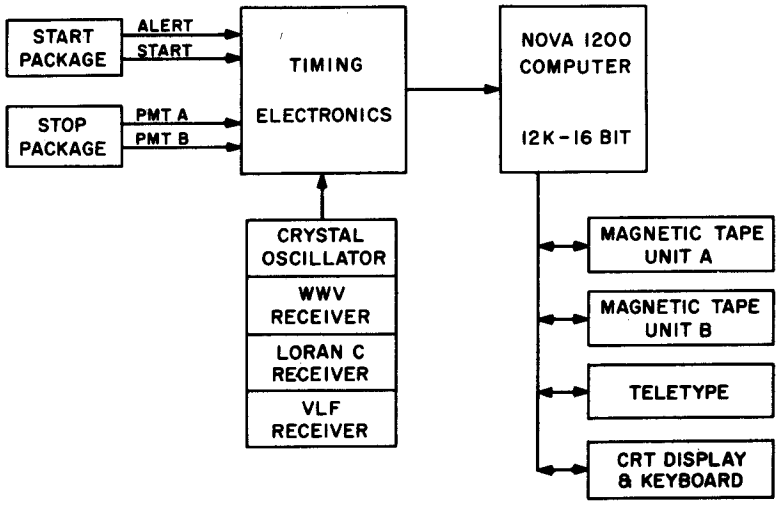

Figure 5. Event Timer System

The crystal oscillator, Austron-Sulzer Model 1250, provides a 10 MHz driving frequency to the event timer unit. The epoch of the event timer is set to UTC via WWVH and Loran C broadcasts, and the frequency of crystal oscillator is monitored and adjusted via Loran C and VLF broadcasts.

The event timer counts the 10 MHz crystal oscillator signal continuously, maintaining epoch to 100 nanoseconds. Events happenings within any particular cycle are timed relative to the end of the cycle by a vernier system. Receipt of an event begins the charging of a capacitor from a constant-current source. The charging continues from the time the event is received until the start of the second following 10 MHz cycle. At the end of the charging period, the capacitor is discharged at a current 125 times smaller than the charging current. The discharge period is measured by an 80 MHz counter that is phase locked to the 10 MHz clock with a resolution of ± 1 cycle. This resolution is equivalent, with the 125 times scaling factor, to 100 picoseconds. The event timer has two independent channels, and each channel can accept 4 events at intervals as short as 20 nanoseconds. The dual channel, multiple event, low dead time features of the event timer allow operation with high background noise and considerable latitude in operating and calibration methods.

The epoch of each event is read by the computer (Data General Nova 1200) and the determination of the type of event and interval between particular events is performed by the computer.

The relatively high repetition rate of the laser, 3 Hz, makes it difficult for an operator to monitor the progress of the ranging operations and decide when a sufficient number of rangings have been recorded for an acceptable measurement. To assist, a histogram of the predicted minus measured range residuals is displayed in real time on a CRT display. The full data set is stored on magnetic tape.

10. Accuracy of Ranges

The uncertainty associated with each range measurement arises from several factors, e.g. the finite laser pulse width, event timer resolution, discriminator walk, and PMT jitter.

Studies conducted at the University of Maryland indicate that PMT jitter is presently the most significant item, with a magnitude of 400 to 500 picoseconds for the best available useful tubes.

The total additional uncertainty contributed by the laser pulse width ($\simeq$ 200 picoseconds FWHM), event timer ($\pm$ 100 picoseconds per event), discriminator walk (100 picoseconds), and other lesser sources may be expected to increase the total uncertainty to 500 - 600 picoseconds per range measurement.

The uncertainty associated with the mean range of N measurements diminishes as the square root of N, making it not unreasonable to achieve an uncertainty of $\pm$ 100 picoseconds for an observation (set of measurements).

11. Conclusions

Current plans are to have the new LURE Observatory operational early in 1974. A staff of 6 to 9 full-time employees will operate the system whenever, during each lunar cycle, background noise and pointing capabilities will allow a reasonable yield of range measurements.

12. References

BUCHROEDER, R. A. 1972. 16-inch f/11 Refractor. Lunar Laser Transmitter System, Design Report prepared for the University of Hawaii, Institute for Astronomy.

CARTER, W. E. 1973. *The Lunar Laser Ranging Pointing Problem*, Department of Civil Engineering, University of Arizona.

FALLER, J. 1972. *The Apollo Retroreflector Arrays and a New Multi-lensed Receiver Telescope*, Space Research XII, Akademie-Verlag Berlin, 211-217.